

Supplemental Information to “Quality control of direct cell-mineral adhesion measurements in air and liquid using inverse AFM imaging”

Abd Alaziz Abu Quba¹, Gabriele E. Schaumann¹, Mariam Karagulyan², Dörte Diehl^{1*}

¹University of Koblenz-Landau, iES Institute for Environmental Sciences, Environmental and Soil Chemistry Group, Fortstr. 7, 76829 Landau, Germany

²Helmholtz Centre for Environmental Research – UFZ, Department of Environmental Biotechnology, Leipzig, Germany

*Corresponding author: Dörte Diehl, diehl@uni-landau.de

Content

SI-1	Characterization and fabrication of the characterizer	2
	Step 1: Blind Tip Reconstruction of potential characterizers	2
	Step 2: Fabrication of characterizers	3
SI-2	Rigidity and accuracy of a characterizer	4
	Rigidity test	4
	Accuracy test	5
SI-3	Light images of the modified probes	7
SI-4	Preparation and characterization of the bacterial coated colloidal probe	7
SI-5	Structure of the kaolinite probe	10
SI-6	Characterization of kaolinite	10
SI-7	The alignment process for inverse imaging	11
SI-8	Height images of the cell-mineral interaction (<i>P. fluorescens</i> -montmorillonite)	12
SI-9	Set-up for systems with potential contamination	12
References	14

SI-1 Characterization and fabrication of the characterizer

Step 1: Blind Tip Reconstruction of potential characterizers

New Sharp Nitride Lever tip (SNL-10, Bruker, USA) was characterized using the Peak Force Quantitative Nanomechanical Mapping (PFQNM) mode in air with an atomic force microscope (AFM, Dimension Icon, Bruker Corporation, USA) by scanning 256-line images over a titanium roughness sample (RS-12M, Bruker, USA), **SI-Figure 1a**. The scan size of 4 x 2 μm and force load of 5 nN were both adapted to have a sufficient number of sharp peaks for analysis, but also to ensure not to blunt the tip. This characterizer was used to study the kaolinite modified probe. The titanium roughness sample was used here because it reflects the shape of very end of the SNL tip (nanoscale) which is important to precisely define the dilation length of the ~ 40 nm thick kaolinite sheets. Calibration of the deflection sensitivity and k of the SNL probe was done by FD curves analysis and the thermal noise method as described in our recent work¹.

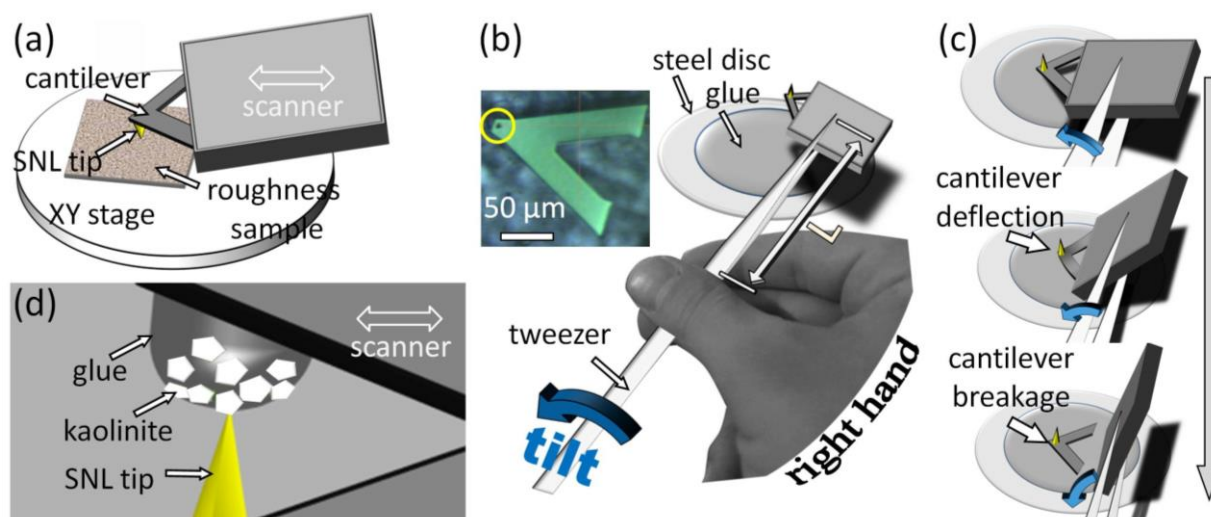
For the bacterial coated tipless probe, we used a Tap150A probe (Tap150A, Bruker, USA) as a characterizer because the tip height is with 10 μm greater than that of the SNL with 4 μm . This was essential to completely scan the larger range of the modified probe. Using tapping mode in air, the Tap150A tip was characterized by imaging 10 x 10 μm (resolution: 512 x 512) square at a TGT1 specimen test grating (TGT1, NT-MDT Spectrum Instruments, USA) that consists of an array of sharp spikes on a Si wafer². Since the bacterial cells are higher (~ 600 nm) compared to the kaolinite sheets, the TGT1 sample was employed to study the overall shape of the Tap150A tip at a sub-micron scale which is essential to explore the cell morphology.

The larger radius of 8 nm of the Tap150A tip in comparison to the 2 nm radius of the SNL tips makes it possible to use the grating system with spikes radii ≤ 10 nm for evaluation. The resonance frequency of the Tap150A probe was obtained using the “Cantilever Tune” function of NanoScope Analysis software (version 8.15, Bruker). An “Auto Tune” with a frequency range that covers the nominal resonance frequency of the Tap150A probe (identified by the producer) was conducted. After identifying the resonance peak, the Tap150A probe was engaged at the grating, the amplitude setpoint was set to be 2/3 the drive amplitude in order to ensure soft tapping and do not damage the tip sharpness.

Using NanoScope software, the resultant images on the titanium roughness sample and grating were flattened by the first order and subjected to blind tip reconstruction analysis in which a total number of peaks greater than 10 were considered. The NanoScope Analysis software evaluates the measured peaks sequentially and defines the rate at which the surrounding Z data slope down. For each new peak, the algorithm updates the shape of the tip at each direction and Z-level only if it is sharper than the previous peak at the corresponding

direction and Z-level. The details of blind tip reconstruction are well discussed by Jozwiak et al.³. By this way, 3-D models of the probes were built which allowed getting important characteristics of the tips, namely, the surface and the face areas at a specific Z level. The former presents the sum of surface areas of the triangles generated between each 3 adjacent raw data points at height (Z) equals or greater than the cut plane level. The face area, however, presents the area of the tip cross-section at the cut plane. The boundary of the cross-section was obtained from a linear extrapolation between the adjacent data points of the respective z height of the cut plane.

If the features in the roughness sample and the grating are not sharper than the measured tip, blind tip reconstruction generates a model of the sharpest domains of the roughness sample. Thus, the sharper the features on the scanned roughness sample the better the 3-D model may reflect the real tip geometry. This highlights an essential limitation of the blind tip reconstruction method if the characterizer is not chosen properly. The titanium roughness sample and the grating sample clearly acted as characterizers in this study because they contain extremely sharp features and have been successfully applied in different studies for estimating such finite probes.⁴⁻⁶



SI-Figure 1. Steps for the preparation of a sharp characterizer: (a) calibration of an SNL tip at a roughness reference sample (tip downward), (b) overview of the required tools and materials for the extraction of the characterizer, (c) inset for steps of extraction sequence up to down (tip is upward, see a video example of this process is in: <https://www.youtube.com/watch?v=0KIK7pqdpLY>), and (d) the “calibrated” characterizer (SNL tip) in use for the investigation of an unknown probe.

Step 2: Fabrication of characterizers

A glue covered steel disc was prepared as described in SI-9. The tip calibrated in step 1 was extracted from its substrate and fixed rigidly on the glue surface to be a characterizer. For this purpose, the probe was held by a tweezers with the right hand, brought under a field of a binocular, and carefully approached the surface of a glue covered steel disc where it should be mounted (**SI-Figure 1b**). Finally, the hand was tilted a bit counterclockwise until the cantilever was broken due to deflection visible as changes in the light reflection (**SI-Figure**

1c). By this approach, the cantilever was placed flat on the surface with an upward directed reference tip (yellow circle in **SI-Figure 1b**). Reducing the distance L between hand and tweezer tips (**SI-Figure 1b**) and holding the breath during the extraction helps diminishing the effect of hand noise.

After the cantilever breakage step, another heat treatment of the glue covered disc with the cantilever was carried out at 38°C for 30 minutes using a heater (MH 15, ROTH, Germany). At this temperature, the glue becomes adhesive which more strongly binds the cantilever, but still remains solid such that the cantilever does not sink inside the glue. Finally, the system is let cool down to room temperature.

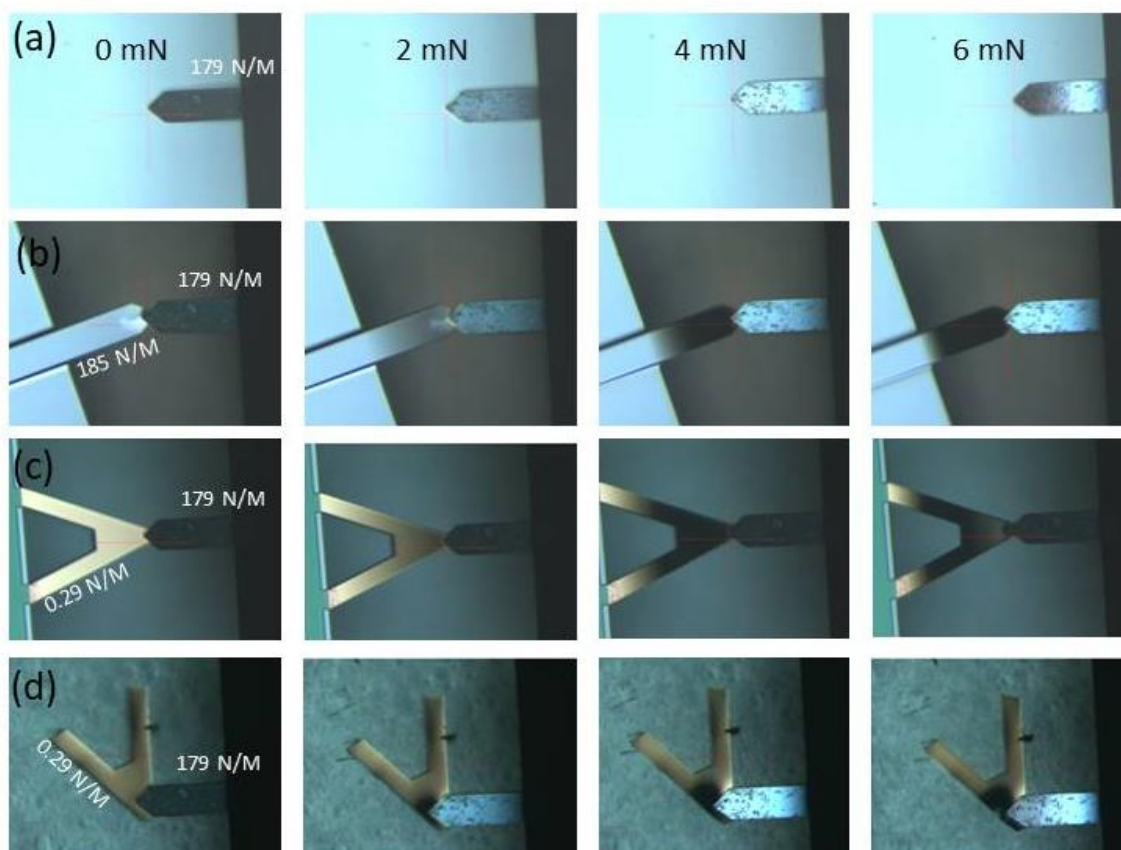
SI-2 Rigidity and accuracy of a characterizer

Rigidity test

A high- k -probe with nominal $k = 200\text{ N.m}^{-1}$ and calibrated $k = 179 \pm 4\text{ N.m}^{-1}$ (RTESP-525, Bruker, USA) was used to compare the deflection on four different samples under loading forces of 0, 2, 4, and 6 mN. The first sample was a sapphire reference (SAPPHIRE-12M, Bruker, USA) representing the hardest surface. The second sample was a high- k -probe with nominal $k = 200\text{ N.m}^{-1}$ and calibrated $k = 185 \pm 3\text{ N.m}^{-1}$ (RTESP-525, Bruker, USA) that was inversely fixed at the sample stage with freely movable cantilever. The third sample was a tipless low- k -probe with nominal $k = 0.03\text{ N.m}^{-1}$ and calibrated $k = 0.029 \pm 0.002\text{ N.m}^{-1}$ (MLCT-O10, Bruker, USA) inversely fixed at the sample stage with freely movable cantilever. The fourth sample was the tipless cantilever extracted from the third sample inversely fixed on a resin glue covered sample disc as described for the characterizer fabrication.

The deflection of the high- k -probe ($k = 179\text{ N.m}^{-1}$) on the sapphire reference surface increased as the load increased from 0 to 6 mN and was visible as changes in the light reflection on the cantilever (from left to right, **SI-Figure 2a**). The same experiment with the sapphire sample replaced by a high- k -probe ($k = 185\text{ N.m}^{-1}$) with freely movable cantilever showed that both cantilevers deflected with increasing load as they carry a very comparable stiffness (**SI-Figure 2b**). Using a ~ 6200 times more flexible low- k -probe ($k = 0.029 \pm 0.002\text{ N.m}^{-1}$) with freely movable tipless cantilever as a sample, only the cantilever of the low- k -probe deflects, whereas a deflection of the RTESP-525 was not detectable (**SI-Figure 2c**). Finally, the deflection experiment was repeated at the cantilever of the same low- k -probe ($k = 0.029\text{ N.m}^{-1}$) after extraction and fixation on a glue covered sample disc (**SI-Figure 2d**). It is evident that the level of deflection of the RTESP-525 on the latter tipless cantilever is qualitatively more comparable to the one on the sapphire surface (**SI-Figure 2a**) than to that on the stiff cantilever (**SI-Figure 2b**). This indicates that a strong rigidity was achieved by this fixation method. Thus, with respect to the μN , nN or pN force range typical for scans on

biological samples, we can fairly assume an infinite spring constant of the characterizer after fixation by our method. Consequently, our aim of combining both, the high-sensitivity of low- k -probes for blind tip reconstruction analysis (**SI-Figure 2c**) and the ultra-high rigidity after their suitable fixation to exclude their deflection when used as a characterizer (**SI-Figure 2d**), is achieved.

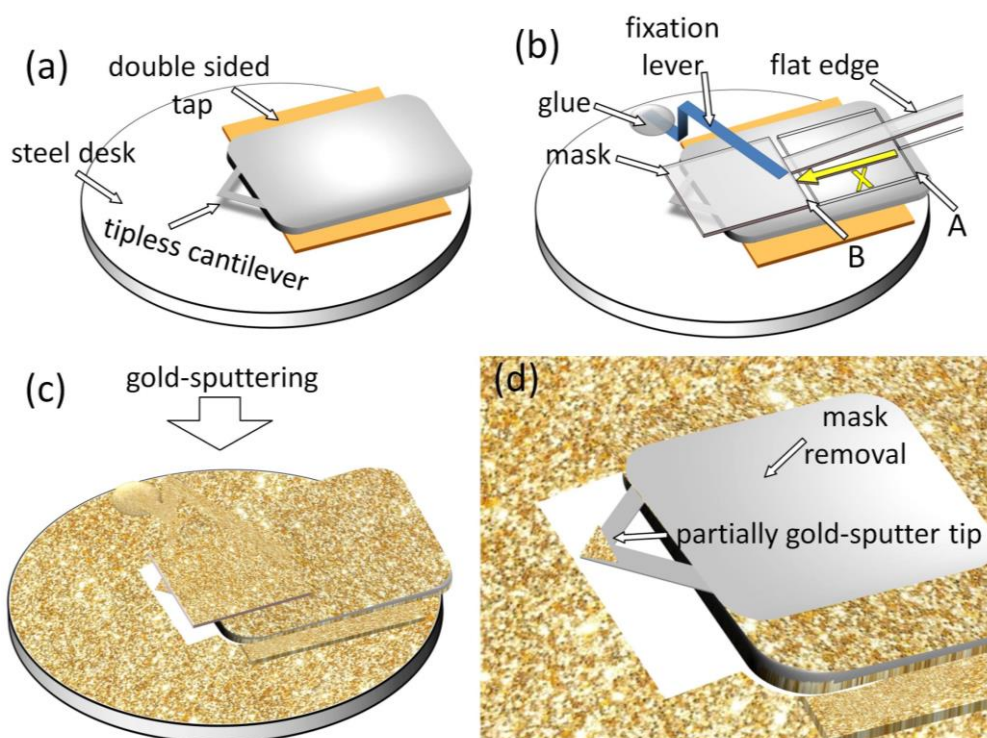


SI-Figure 2. Deflection test made in order to test the stability of the characterizer extracted by our method, (a) a high- k -probe attached to the AFM holder deflects against a sapphire surface using increasing loads from left to right images (deflection is visible as changes in the light reflection of the probe), (b) the deflection test is made against another high- k -probe, (c) the deflection test is made against a low- k -probe, and (d) the deflection test is made at the same probe in (c) after the extraction and fixation on the glue surface. The very flexible tipless probe in (c) turned to a very stiff after the fixation on the glue surface (d) which means that we succeeded in having a flexible probe for an accurate blind tip reconstruction analysis and a stable characterizer for a reliable inverse imaging process.

Accuracy test

A tipless cantilever ($k = 0.03 \text{ N.m}^{-1}$, MLCT-O10, Bruker, USA) was partially sputtered with Au ions to introduce as much nano-irregularity as possible and study the resultant rough and complex patterns in the cantilever plane. The results of inverse imaging at a sharp characterizer were compared with ESEM pictures and with inverse imaging at a blunt tip to highlight the importance of studying the quality of the characterizer tip in advance.

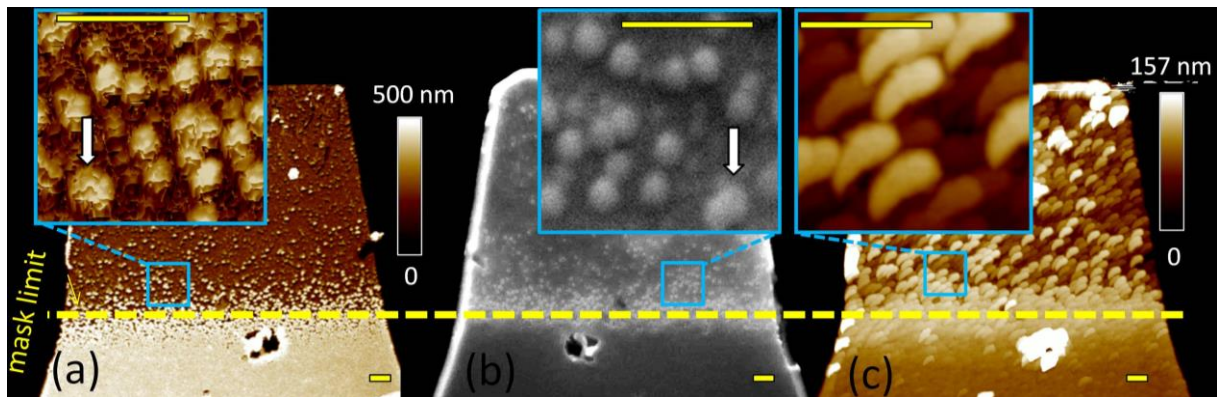
Prior sputtering, the backside of the substrate was glued to a double-sided adhesive tape (**SI-Figure 3a**). Afterward, a mask was put onto the front side of the substrate at position “A” and carefully shifted by “X” into position “B” partially covering the cantilever (see A, B, X in **SI-Figure 3b**). During the displacement, the mask was introduced underneath a fixation spring that pressed the former against the substrate ensuring an immobile system for coating. The tool which was used to move the mask has a flat edge and was fixed at a custom made XYZ navigation system driven by micrometer screws. The gold sputtering (**SI-Figure 3c**) was performed using a Quorum Q150R Rotary-Pumped Sputter Coater (Quorum Technologies, Lewes, United Kingdom) with 20 mA as deposition current and 1×10^{-1} Mbar as pressure for 60 minutes with two short pauses after 20 and 40 minutes to eliminate thermally activated processes. After sputtering, the mask was carefully removed revealing a partially gold sputtered cantilever (**SI-Figure 3d** and **a**).



SI-Figure 3. Preparation steps for the sputter coating: (a) substrate glued to a double-sided adhesive tape onto a steel disc, (b) positioning of a mask above the substrate to partially cover the cantilever, (c) sputtering process, and (d) cantilever after sputtering and removal of the mask.

The inverse image of the sputter-zone above the mask limit is characterized by rough dots with an average diameter of 180 nm as shown by the inset (**SI-Figure 4a**). Comparison with the mirror-inverted ESEM image (white arrows indicate an identical particle) of the same regions (**SI-Figure 4b**) shows that AFM produces a superior and clearer image with sharper details at the nanoscale than ESEM may give. However, using a blunt tip as a characterizer, the image is dominated by “banana-like” structures reflecting the shape of the blunt tip of the used characterizer rather than the details of the sputtered coated probe (**SI-Figure 4c**). Therefore, it is essential to study the quality of the tips before their use as characterizers. As a

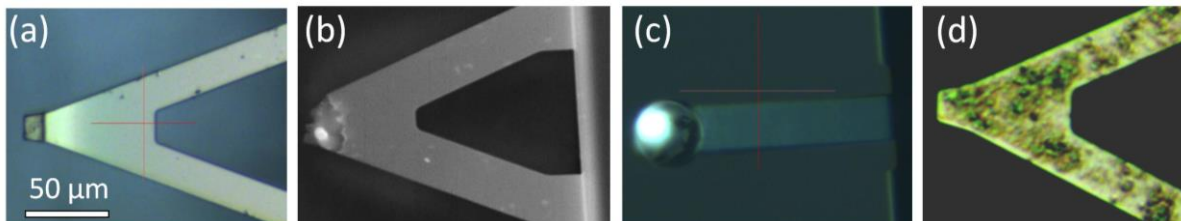
consequence, our method enables a precise investigation of the modified probes with a resolution limited only by the sharpness of the chosen characterizer.



SI-Figure 4. (a) Inverse image of the gold sputtered probe made at a new sharp characterizer. The yellow dashed line presents the mask limit above which the sputter was achieved. The blue frame shows inset of nanostructure above the mask, (b) same as (a) using ESEM, (c) same as (a) using inverse imaging at a non-sharp characterizer (blunt tip). The “banana-like” patterns represent the shape of the bluntness of the used tip. It is evident that the AFM image (a) is superior compared to ESEM (b) for determining the sharp details at the nano-scale. Scale bar 400 nm.

SI-3 Light images of the modified probes

All modified probes were imaged by the light microscope integrated to our AFM. It is clear that they hold various shapes and tip structures which we aimed to prove the capability of the proposed inverse imaging method (**SI-Figure 5**).

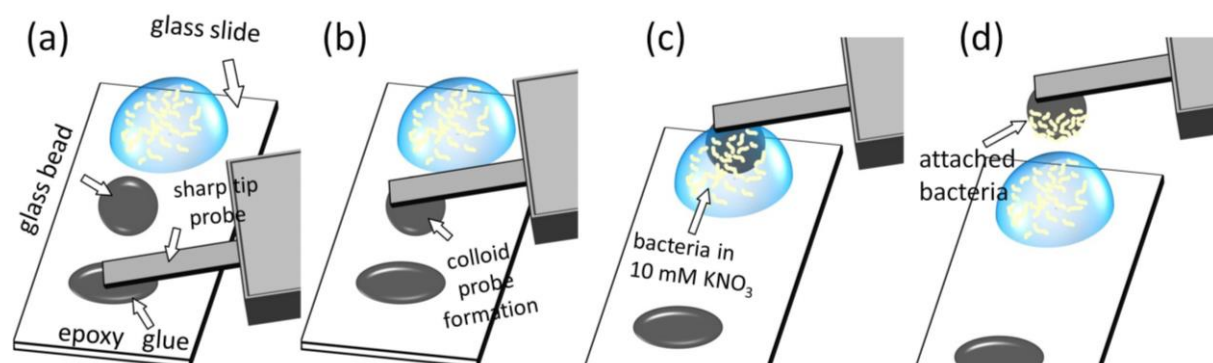


SI-Figure 5. Light images of the modified probes studied by the inverse imaging method proposed in this work, (a) gold-sputtered-tipless-probe, (b) SNL probe modified by adding glue at the end, (c) colloidal and (d) tipless probes covered with bacteria.

SI-4 Preparation and characterization of the bacterial coated colloidal probe

A colloidal probe was prepared by attaching a glass bead (GB2000, soda lime, MHG Strahlanlagen GmbH, Germany) at the end of a probe with a sharp tip ($k = 2 \text{ N.m}^{-1}$, AC240TS-R3, Oxford Instruments, USA) using epoxy glue (Pattex Kraft Mix, Henkel AG, Germany). The large diameter of the glass bead $40 \mu\text{m}$ in comparison to the AC240TS-R3 tip height ($9\text{-}20\mu\text{m}$) ensures that the glass bead is more prominent. However, the tip at the end of the probe enhances the contact area with the glass bead making the colloidal probe more

stable. Using the AFM XYZ navigation system, the probe was driven into the glue spot (**SI-Figure 6a**) to get some glue at its end. Then, we directly moved the probe to contact the glass bead and waited 3 minutes to enhance the fixation (**SI-Figure 6b**). The produced colloidal probe was then cleaned by immersing it several times subsequently in ethanol and in Milli-Q water before modifying with bacteria by immersing it three times in a *P. fluorescens* suspension with an optical density (OD) of 0.9 (**SI-Figure 6c**) and shortly air drying to form a bacterial film (**SI-Figure 6d**). We finally immersed the probe in 10 mM KNO₃ several times to remove loosely attached cells.

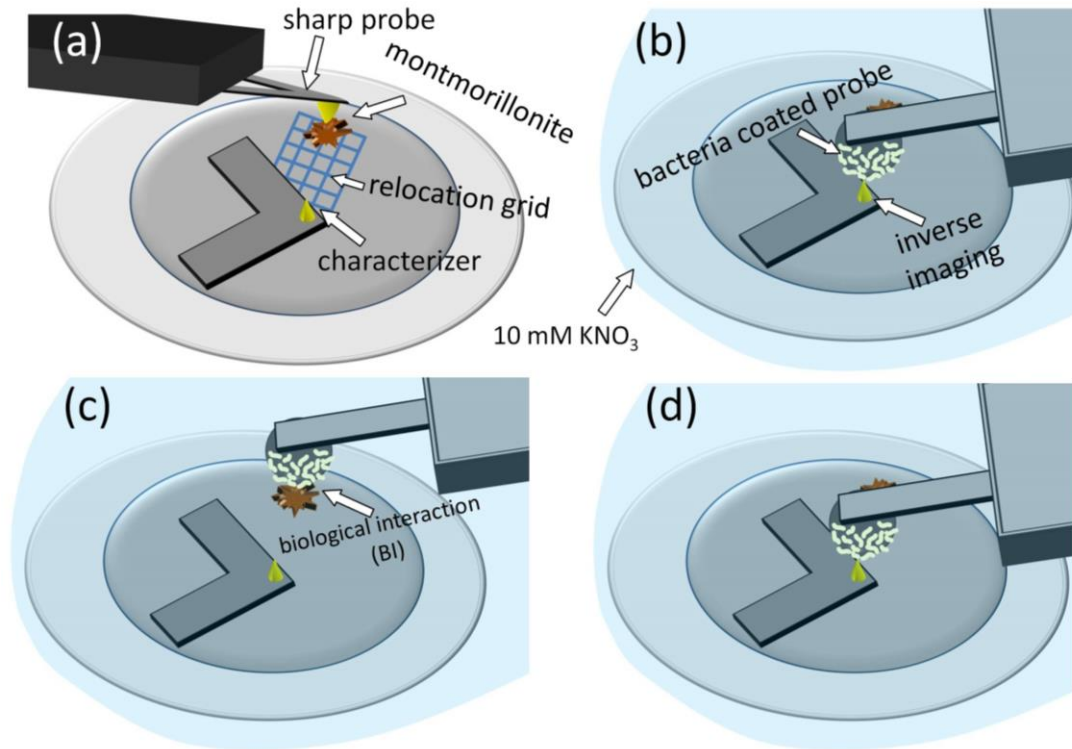


SI-Figure 6. Preparation steps for the bacterial coated colloidal probe: (a) a sharp tip probe gets in contact with an epoxy glue spot, (b) positioning the end of the probe over a micro-sphere, (c) immersing the colloidal probe in a highly concentrated bacteria suspension and (d) retracting from the bacteria droplet and waiting some minutes to adhere the cells.

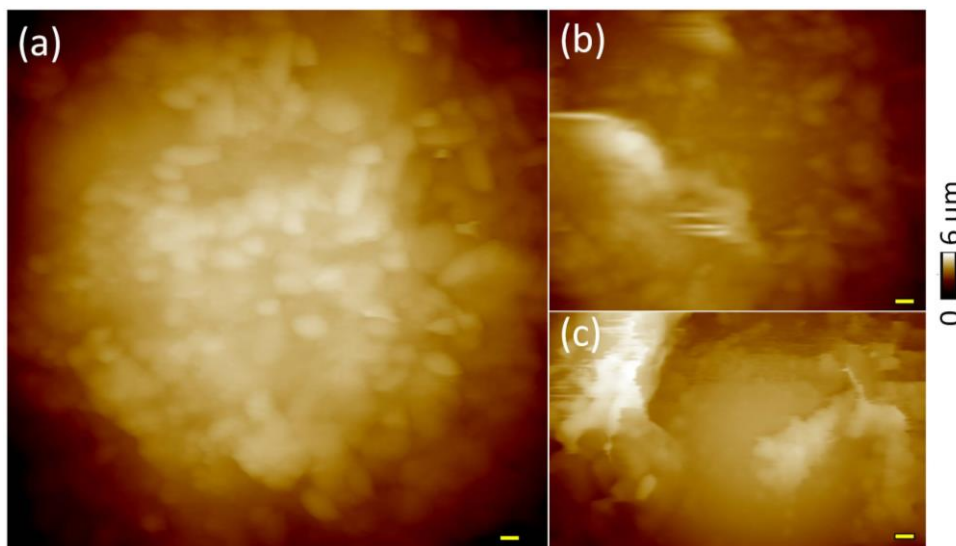
To calibrate it, the modified probe was used to obtain FD curves on the built-in characterizer in air. The FD curves were analyzed as described in our work¹ in order to get the deflection sensitivity which allowed getting k by the thermal noise method. Finally, the deflection sensitivity was once again calibrated after introducing the modified probe into the KNO₃ solution.

For the cell-mineral interaction, a selected montmorillonite particle was imaged by a sharp probe in air (**SI-Figure 7a**). Then, the bacterial coated probe was introduced to 10 mM KNO₃ environment and inversely imaged at the built-in characterizer, **SI-Figure 7b**. Afterward, cell-mineral interaction between the bacterial probe and the montmorillonite particle was obtained using PFQNM mode at 5 nN (**SI-Figure 7c**). A subsequent check of the bacterial probe was realized in order to test the stability of the modified probe (**SI-Figure 7d**).

The inverse image of the bacterial probe showed that the spherical tip is originally evenly covered with bacteria (**SI-Figure 8a**). However, after the cell-mineral interaction the microbial coverage was removed from the tip apex (**SI-Figure 8b**). **SI-Figure 8c** shows an example of a bacterial probe that was unsuccessfully modified and thus not used for cell-mineral interaction. Thus, we suggest modifying the colloidal probe first with positive charges such as using poly-l-lysine (PLL) to enhance the adhesion of bacteria.⁷



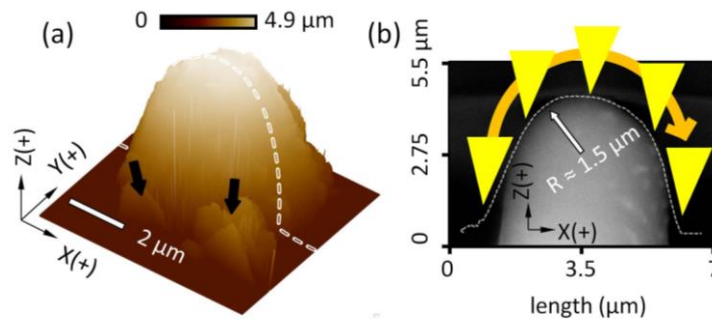
SI-Figure 7. Setup of the cell-mineral interaction experiment between the bacterial coated probe and montmorillonite: (a) a montmorillonite particle is studied by a sharp probe, (b) bacterial probe is inversely studied at a sharp built-in characterizer, (c) using the relocation grid, the same montmorillonite particle is scanned by the bacterial probe and (d) subsequent check of the state of the bacterial probe at the characterizer.



SI-Figure 8. Case study of the influence of cell-mineral interaction on the state of bacterial probe, (a, b) inverse images of a bacterial probe before and after a cell-mineral interaction with a montmorillonite particle, respectively, and (c) an image of another bacterial probe inhomogeneously coated with bacteria after the modification process which was therefore not used for cell-mineral interaction. By comparison between (a) and (b), it is clear that the bacterial colony is removed from the tip apex after the cell-mineral interaction indicating a wrong strategy of bacterial fixation. Scale bar 500 nm. All images were made in KNO_3 ; which was also used for cell-mineral interaction (not shown).

SI-5 Structure of the kaolinite probe

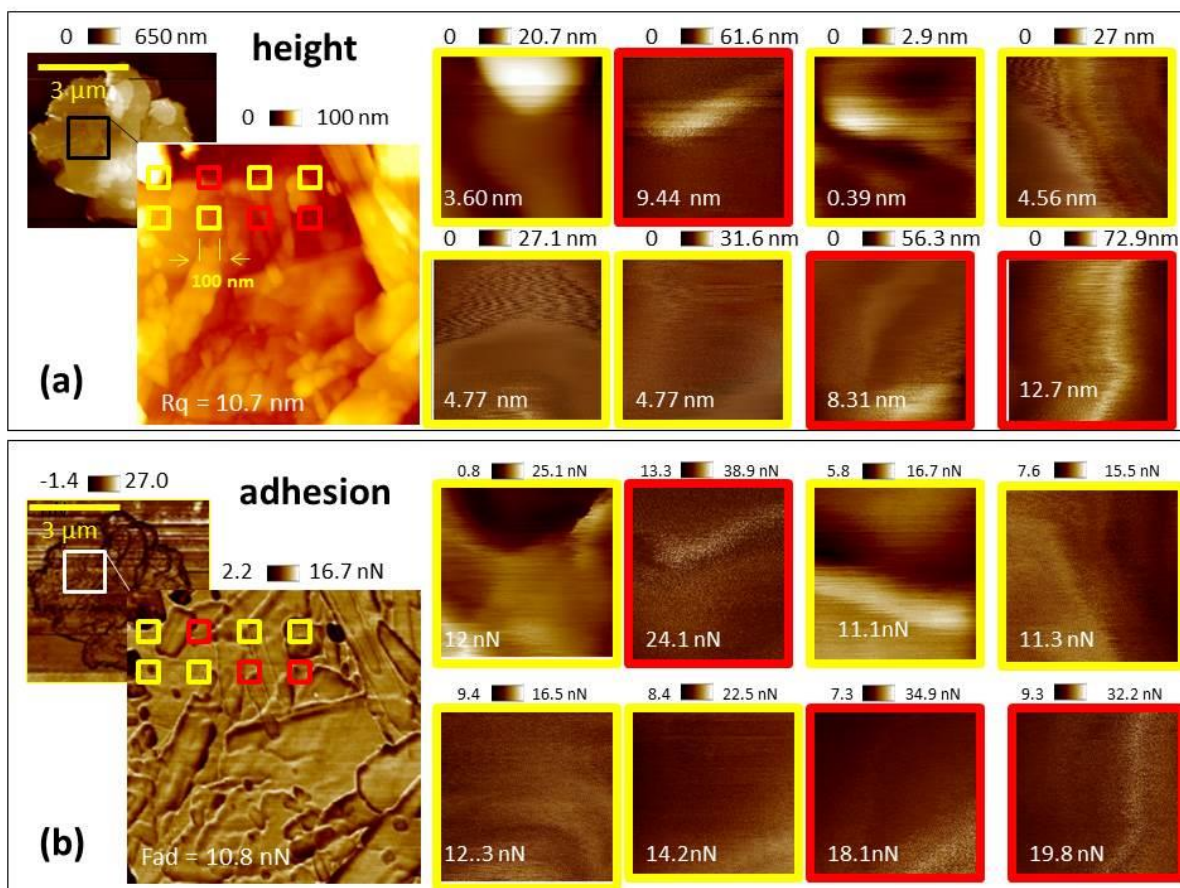
The inverse image obtained from the scan of the kaolinite probe over the built-in characterizer revealed a height of the modified tip of approximately $4\ \mu\text{m}$ (**SI-Figure 9a**). Due to the withdrawal process during the preparation of the modified tip, the glue formed a round drop-like shape at the cantilever end (**Figure 1a** in main article). In order to evaluate the mechanical stability of the glue body during AFM interaction, a line-scan of its profile (white line in **SI-Figure 9a**) was superimposed with an ESEM image of the probe (**SI-Figure 9b**). The excellent agreement between the profiles in the upper part of the glue represents essential evidence that the glue is stable enough and does not deform during AFM scans. However, a deviation found at lower Z range is likely attributed to the tip-sample convolution as demonstrated by the positions of the characterizer tip during a line scan (yellow sketches in **SI-Figure 9b**).



SI-Figure 9. (a) 3D-view of the kaolinite probe showing some kaolinite clusters trapped at the base of the glue-tip (arrows), (b) comparison of the probe profile obtained by ESEM and AFM (dotted line in (a)). The two techniques show a great match at the tip-apex, but they deviate in the surroundings due to convolution between the characterizer and glue geometries.

SI-6 Characterization of kaolinite

To ensure that the fabrication of the kaolinite probe (Section 2.4 in main article) did not induce contaminations, e.g. dust, we compared the adhesion of the small kaolinite cluster attached at the top of the modified probe with the adhesion of a “larger (and thus more distinguishable)” kaolinite particle attached on tempfix glue surface (as described in our work¹). The good agreement between the two SNL tip radii (the one used as a characterizer of the kaolinite probe and the one used to scan the kaolinite particle fixed at the glue surface) allowed a direct comparison of adhesion forces with no need to normalize the forces over the contact areas. The average adhesion of 8 local areas within the particle ($15.36 \pm 4.78\ \text{nN}$, **SI-Figure 10b**) was of a good agreement with the value obtained at the kaolinite cluster attached to the modified probe ($13.25 \pm 1.34\ \text{nN}$). A small deviation would be attributed to geometrical aspects. More specific, one can see that the mean adhesion rises up when R_q increases leading to a slight increase of the average adhesion (see red frames in **SI-Figure 10b** and **a**, respectively).



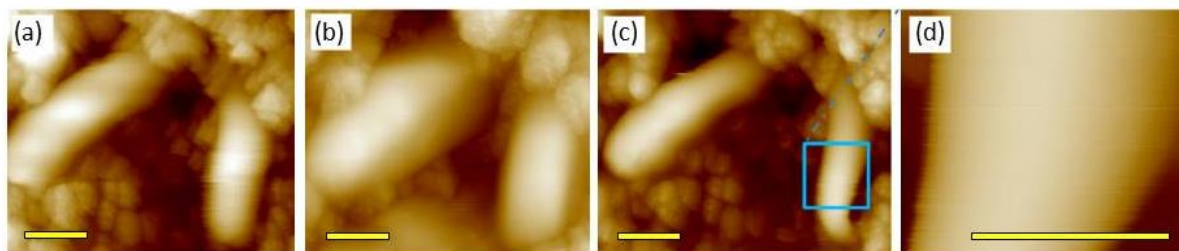
SI-Figure 10 (a) height channels of a matrix of 8 local areas inside a single kaolinite particle shown by the two images in the left side. The number in white color presents the mean Rq value for each area, (b) the adhesion channels corresponding to the height channels in (a). The number in white presents the mean adhesion force for each area. The rougher the topography is, red frames in (a), the higher the adhesion is, red frames in (b).

SI-7 The alignment process for inverse imaging

The alignment of the kaolinite probe over its built-in characterizer was realized by the engagement of the kaolinite probe at the characterizer cantilever. Then the kaolinite probe was driven towards the tip of the characterizer introducing X and Y offsets. The scan angle was set to 90° while the scan rate was minimized to 0.1 Hz in order to reduce the lateral forces. The feedback gain was raised from 5 to 50 in order to let the feedback run fast and accumulate for the high rate of Z changes as soon as the kaolinite probe starts climbing at the pyramid edges of the characterizer and up to the point when it reaches the central position. By subsequent scans, the scan angle was kept at 90° , the feedback gain was set back to 5, whereas the scan speed varied. For the colloidal probe system, the center of the sphere of the bacterial probe was engaged at the tip of its built-in characterizer and then fine X and Y tuning was done during imaging to reach the apex of the spherical tip. Finally, the alignment of the bacterial coated tipless cantilever was done by its direct engagement at the tip of the

built-in characterizer which is the same strategy used to align the sputtered probe at its characterizer.

SI-8 Height images of the cell-mineral interaction (*P. fluorescens*-montmorillonite)



SI-Figure 11 (a, b, c, d) Height images of Figures 3(h, b, k, m) in the main article, respectively. In line with the Error channels, a change of the shape of right cell (c) compared to the case before (a) is evident. Scale bar 400 nm. Height scale 0 - 600 nm. Images were made in 10 mM KNO_3 .

SI-9 Set-up for systems with potential contamination

In case the liquid environment used for the cell-mineral interaction contains loosely bound, or freely moving, particles and cells which may bind to the exposed surfaces, it is important to study the characterizer before and after the cell-mineral interaction to ensure that it remains intact.

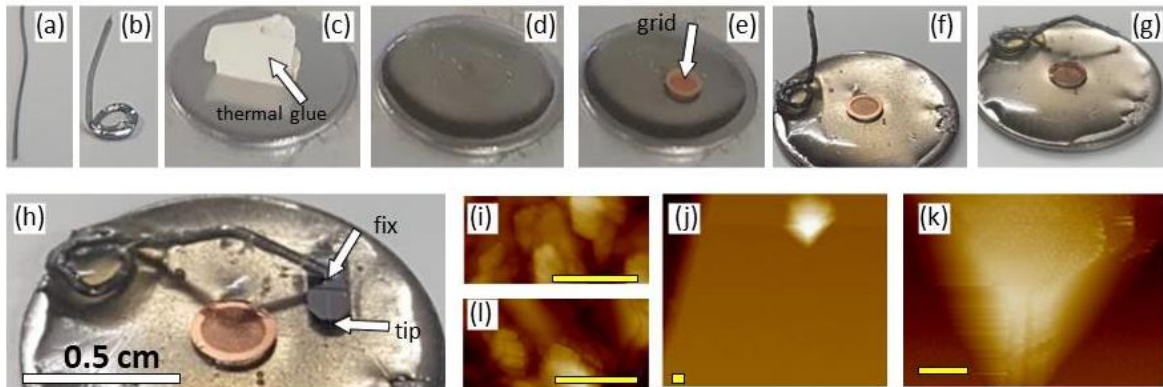
Here, we made a set-up that allows adding and removing the characterizer from the relocation system which, in turn, enables qualifying the characterizer tip before and after the cell-mineral interaction.

First, a 2 cm long elastic metallic wire is cut and bent from the bottom, **SI-Figure 12a** and **b**, respectively. Then a small piece of tempfix glue is put over a steel disc which was heated up to 130°C for 4 minutes melting the glue, **SI-Figure 12c** and **d**, respectively. While the system was still hot, a relocation grid, **SI-Figure 12e**, as well as the metallic wire, **SI-Figure 12f**, were added. After moving the system away to cool down (for ~ 2 minutes), the metallic wire was bent to form a fixation lever which holds the substrate of the characterizer as shown in **SI-Figure 12h**. The probe used here is RTE525 with calibrated $k = 183 \pm 3 \text{ N.m}^{-1}$.

In order to test the system, we made the following experiment: first, the RTE525 probe was attached to the AFM holder and used to make a tapping mode image of the titanium roughness sample, **SI-Figure 12i**. Then, the probe was inversely fixed at the relocation system i.e. with tip upward, **SI-Figure 12h**. After attaching the system to the AFM stage, a new SNL-10 probe with $0.35 \pm 0.05 \text{ N.m}^{-1}$ was attached to the AFM holder and imaged the tip of the RTE525 probe using PFQNM mode in Milli-Q water, **SI-Figure 12j** and **k**. After letting the system to air dry, the RTE525 probe was removed from the relocation

system and used to make another tapping mode image of the roughness sample, **SI-Figure 12l**. The tip-tip interaction addressed in **SI-Figure 12k** was made to demonstrate the stability of the built-in characterizer against high lateral forces.

In general, one can see good agreement between the images made at the roughness sample which allows excluding that the RTESP-525 is contaminated, **SI-Figure 12i** and **l**. It should be noted that this system works provided that the characterizer carries much higher spring constant compared with the modified-probe (in this example represented by the RTESP-525 and the SNL-10, respectively).



SI-Figure 12 (a) a 2 cm long elastic wire which (b) is bent from the bottom, (c) a small piece of the thermal glue is placed over a steel disc which (d) is heated melting the glue, (e) a relocation grid and (f) the elastic wire are added while the system is still hot, (g) the elastic wire is bent forming a fixation lever after cooling the system to room temperature, (h) a characterizer with high spring constant is fixed under the fixation lever, (i) an image of the titanium roughness sample made by the characterizer before the introduction to the relocation system in (h), (j) inverse image made by the characterizer fixed in the relocation system as in (h) against an SNL probe attached to the AFM holder in water, (k) inset inside (j) showing the pyramid SNL tip and (l) an image of the roughness sample made by the characterizer after the investigation addressed in (j, k). Scale bar 400 nm. Height scale 0 - 100 nm for (i, l), 0 - 10.2 μm for (j) and 0 - 7.6 μm for (k). This method enables removing the characterizer from the relocation system to check its state after use which is important for measurements in liquid environments with potential contamination. Nevertheless, the method is restricted to high spring constant characterizers.

References

1. Abu Quba, A. A., Schaumann, G. E., Karagulyan, M. & Diehl, D. A new approach for repeated tip-sample relocation for AFM imaging of nano and micro sized particles and cells in liquid environment. *Ultramicroscopy* **211**, 112945 (2020).
2. Bosse, J. L. & Huey, B. D. Error-corrected AFM: a simple and broadly applicable approach for substantially improving AFM image accuracy. *Nanotechnology* **25**, 155704 (2014).
3. Jozwiak, G. *et al.* The regularized blind tip reconstruction algorithm as a scanning probe microscopy tip metrology method. *arXiv:1105.1472 [physics]* (2011).
4. Huang, Q., Yoon, I., Villanueva, J., Kim, K. & Sirbully, D. J. Quantitative mechanical analysis of thin compressible polymer monolayers on oxide surfaces. *Soft Matter* **10**, 8001–8010 (2014).
5. Khadka, N. K., Teng, P., Cai, J. & Pan, J. Modulation of lipid membrane structural and mechanical properties by a peptidomimetic derived from reduced amide scaffold. *Biochim Biophys Acta Biomembr* **1859**, 734–744 (2017).
6. Yu, X., Burnham, N. A., Mallick, R. B. & Tao, M. A systematic AFM-based method to measure adhesion differences between micron-sized domains in asphalt binders. *Fuel* **113**, 443–447 (2013).
7. Doktycz, M. J. *et al.* AFM imaging of bacteria in liquid media immobilized on gelatin coated mica surfaces. *Ultramicroscopy* **97**, 209–216 (2003).